TOWARDS A VIRTUAL CHARACTERIZATION OF A BIAXIAL NON-CRIMP FABRIC

David Colin[1], Sylvain Bel[2], Thorsten Hans[3], Mathias Hartmann[1]

[1]Technical University of Munich, TUM Department of Mechanical Engineering, Chair of Carbon Composites, Boltzmannstraße 15, 85748 Garching, Germany
Email: colin@lcc.mw.tum.de, Web Page: http://www.lcc.mw.tum.de/en/home/
[2]LMC2, Université Lyon 1, 82 Blvd. Niels Bohr, Domaine Science DOUA, 69622 Villeurbanne Cedex, France
Email: sylvain.bel@univ-lyon1.fr, Web Page: http://lmc2.univ-lyon1.fr
[3] KDX Europe Composites R&D Center GmbH, Am Weiglfeld 15, 83629 Weyarn, Germany
Email: Thorsten.Hans@kdx-erd.com, Web Page: http://kdx-erd.com

Keywords: Non-crimp fabric, Microscopic modeling, Virtual testing, Representative unit cell, Finite element analysis (FEA)

Abstract
Non-Crimp Fabrics (NCF) are widely used due to their enhanced mechanical properties. However, the manufacturing process of this textiles involves many parameters that influence the mechanical behavior of the dry preforms. Studies on the stitching patterns, stitching length or gauge have been conducted to investigate the overall textile deformability. However, in order to predict the behavior of the NCF appropriately, the deformation mechanisms occurring at refined scales should be accurately reproduced. The present study proposes a finite element description of a 0/90° biaxial tricot-chain stitched NCF to virtually investigate its mechanical behavior on a repetitive unit cell. A method to model the manufacturing process starting from a homogeneously distributed fibrous mat is proposed. The resulting virtual description of the textile correlates well with the geometry of the NCF. Virtual characterization of the compaction and shear behavior is subsequently performed and compared to experimental results. The deformation kinematics are well reproduced but the idealization of the fibrous mat leads to reduced inter-fiber interactions.

1. Introduction

Multilayer multiaxial Non-Crimp Fabrics (NCFs) are very attractive for the automotive industry due to their superior stiffness compared to woven textiles, while offering good handling capabilities. During the manufacturing process of NCFs, the fibrous mat of the layers are stitched together using various patterns. Therefore, the deformation behavior of the textile does not only depend on the orientation of the layers but also on the stitching that should be accounted for in the description of the deformation kinematic [1]. The drapeability of a textile is characterized by its ability in accommodating three-dimensional geometries through bending and shear deformation without defects such as wrinkles or fiber waviness. The sewing process parameters influence drastically the deformability of the textile. For example, NCFs with a tricot pattern exhibit a textile structure with more loosely tows compared to the chain-loop pattern, which leads to a better drapeability [2]. Moreover, multilayer multiaxial NCF possibly exhibit asymmetrical shear behavior, depending on the combination of stitching length and stitching gauge, defined as the distance between the stitching loops in the machine direction and the spacing between the needles, respectively [3]. In order to study further the properties of this textile, one should focus on the deformation mechanisms. To that end, Creech and Pickett [4] presented the deformations at the mesoscopic scale (scale of a tow), that can be gathered in three groups: the deformation of the fibrous mat, the deformation of the stitching yarn, and the interaction between them. Moreover, Colin et al. [5] showed the occurrence of a significant inter-stitch sliding during shear deformation and pointed out the relevance of this deformation mode to be included in models at the scale of fibers or group of fibers.

The present study aims at a virtual representation of a biaxial NCF to study its deformation mechanisms. The finite element model description is implemented at the scale of group of fibers, leading to a discretization of the tows in many groups of fibers. First the modeling principle to generate and reproduce the studied biaxial NCF is proposed. Then, the simulation procedure to generate a virtual description of the NCF referred to as the "as-manufactured" geometry is described. Virtual tests are subsequently performed and compared to experimental results to validate the accuracy of the model and the accuracy in predicting the mechanical behavior of the textile.

2. Model description

The material used for this study is a biaxial 0°/90° NCF from SGL KÜMPERS® (HPT 310 – C090 (90°//0°//P)). The stitching pattern of this NCF is a tricot-chain pattern with a stitch gauge and stitch length of 5.08 mm and 2.8 mm respectively, cf. Fig. 1. As described before and according to Harrison et al. [6], models aiming at predictive capabilities should accurately reproduce the mechanical behavior of the fibers or group of fibers. Due to the high level of details, a whole textile sample cannot be fully modeled. Therefore, a Repeating Unit Cell (RUC) of the textile should be modeled with adequate boundary conditions to reproduce the behavior of the whole material. Many examples have been published on RUCs of woven fabrics [7], 3D-woven fabrics [8], biaxial braids [9] or NCF [10]. The stitching pattern used to produce the present NCF repeats after 4 knitting cycles. Therefore, the smallest RUC as illustrated in Fig. 1 is 5.08 mm wide and 11.2 mm long. Periodic boundary conditions are applied on the model. The mesoscopic periodicity of the textile is therefore transferred to a refined level, leading to the assumption of fibers perfectly aligned between opposed edges of the RUC. Therefore, the variability in the fiber alignment or in the size of the tows (as it can be observed in Fig. 1) cannot be reproduced in the model. This assumption will be discussed in the following.

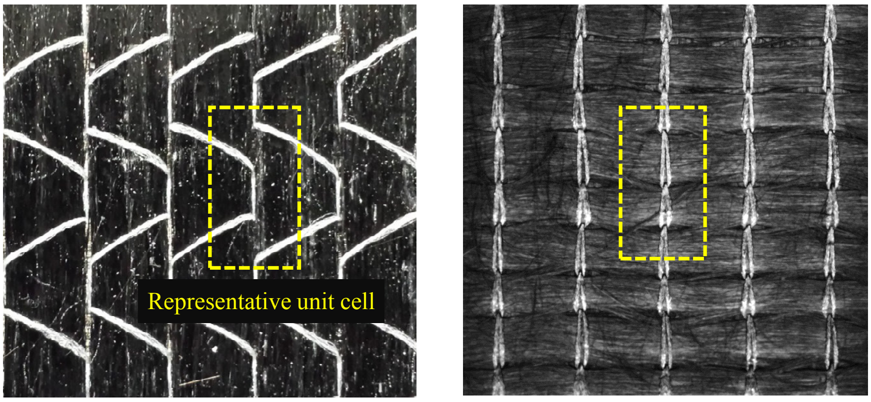

Figure 1. Illustration of the representative unit cell on the front face (left) and back face (right) of the 0°/90° biaxial tricot-chain stitched NCF.

In order to model the fibers or group of fibers, one can first neglect their bending stiffness and consider that the rigidity of the textile results only from frictional forces. Thereby, the fibers are modeled with rod-elements connected with frictionless pins, often referred to as "digital chain elements" [11,12]. The frictionless articulation between the rod-elements ensure a free rotation at the connecting nodes. As a result, a perfect flexibility of the whole chain is only ensured if the length of the elements is very small. A microscopic model with beam elements accounting for a bending stiffness of the fiber bundles has been proposed by Green et al. to model the compaction behavior of 3D woven preforms [8]. However, modelling many fibers in one element would lead to an overestimation of the bending stiffness. To tackle this problem, Green et al. used an elastic perfectly-plastic model in order to reduce the bending stiffness of the bundles after a given deflection. The simulation results correlated well with Computer Tomography (CT) scans but the model principle is not able to reproduce the forces in the woven fabric when deformed. Moreover, the results sensitively depend on the yield strength used to reduce the bending stiffness, which is not a physical parameter. This modelling principle has also been used by Thompson et al. [10] to predict the mesoscopic geometry of the tows of a biaxial 0°/90° NCF. An enriched kinematic beam model was presented by Durville [13] in order to account for planar deformation of the cross-section of the fiber bundles. However, an implicit integration scheme is used here, which requires intensive development efforts of the contact algorithms to reach a reasonable convergence rate and calculation time with commercial FE solvers. In the present study, elements corresponding to the description of the digital chain elements presented by Zhou et al. [11] are used with the solver Abaqus/Explicit (the rods only deform in the axial direction without bending deformability).

The tows are discretized in many groups of fibers, referred to as “multi-chain model”. The contacts between the digital chain elements is modelled with coulomb friction. A coefficient of 0.3 is assumed in the whole model. In order to generate comparable models with varying tow discretization, the diameter of the digital chains is calculated such that the total volume of the fibers is kept constant. Although the stitching yarns are constituted of many filaments, they are modeled with only one single digital chain, leading to a comparable discretization size of the tows. Since truss elements assume a constant cross section, the model accuracy may be reduced where the stitching yarns are flattened, typically on the top and bottom of the NCF [14].

3. Generation of the “as-manufactured” geometry

The manufacturing process needs be accurately reproduced in order to generate a realistic “as-manufactured” geometry. Zhou et al. proposed a solution applied to woven fabrics where the weaving process of the warp and the weft is reproduced step by step [11]. However, the stepwise model generation leads to high computation time. Another possibility widely adopted in the literature is to start from an idealized geometry and apply an adequate load to reach the realistic geometry. In that way, Wang et al. presented a dynamic relaxation of an idealized geometry of a 3D woven fabric. Starting from an idealized representation of the weaving pattern, tension is applied to the yarns and relaxed to reach an accurate microscopic geometry [12]. Thompson et al. presented a virtual description of a biaxial 0°/90° NCF with predefined gaps between the tows and applied a progressive negative temperature on the stitching yarn to obtain the as-manufactured geometry [10]. In this paper, a mixed method is proposed.

The fibers of both layers (0° and 90°) are first homogeneously distributed to model the fibrous mat before the sewing process. The thickness of the NCF material is a priori not known and is directly linked to the Fiber Volume Fraction (FVF) as follow:

$$V_f * t * \rho_{\text{fibers}} = A \tag{1}$$

Where t corresponds to the thickness and A the areal weight of the fibrous mat, V_f the fiber volume fraction and ρ_{fibers} the density of the fibers.
An initial FVF $V_f = 0.3$ is considered for the generation of the idealized fibrous mat. Models generated with various tow discretization are illustrated in Figure 2.

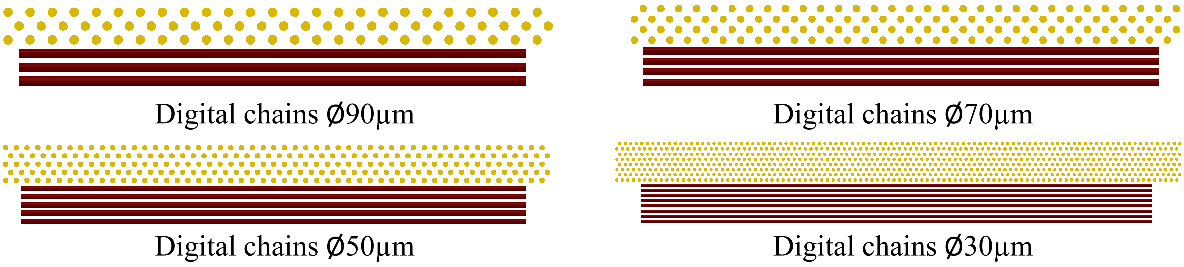

Figure 2. Model of the fibrous mat for various tow discretization with constant fiber volume fraction.

The stitching yarns should be subsequently introduced in the model. Since the chain elements are homogeneously distributed over the modeled unit cell, an interpenetration between the stitching yarns and the digital chains occurs at the beginning of the simulation. A first step is therefore required to set the contact between the fibers and the stitching yarn and resolve the interpenetration. To that end, the sewing process is modelled with needles that move the fibers apart when they penetrate the fiber bed as illustrated in Fig. 3a). Subsequently, the stitching yarns are idealized using sharp edges at the location of knitting points left by the needles (see Fig. 3b). Since the chain elements are free to rotate, this sharp geometry does not induce stress concentrations at their corners. In the following simulation step, the contact between the stitching yarn and the fibers is set. A negative thermal load is subsequently applied to the stitching yarn, which are modeled with a thermal expansion coefficient, to reproduce the tension induced by the knitting unit during the sewing process. The result of the second simulation step after pretension of the stitching yarn is presented in Fig. 3c).

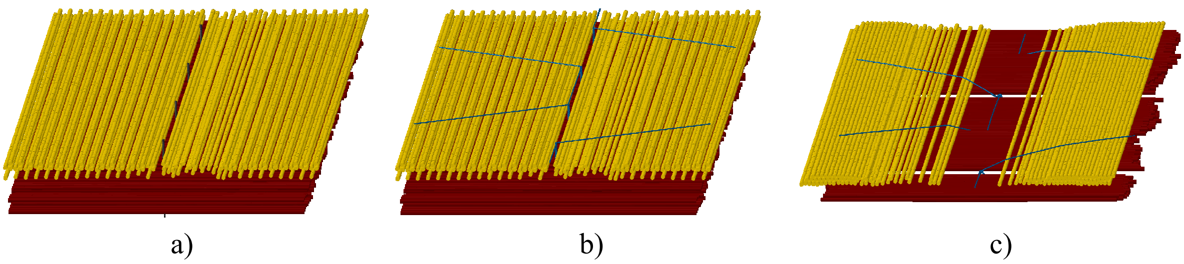

Figure 3. a) Penetration of the fiber bed, b) idealization of the stitching yarn geometry, c) and simulation result after the pretension of the stitching yarns.

The geometry illustrated in Fig. 3c) is repeated in the direction of periodicity. The virtual "as-manufactured" textile is compared in Fig. 4 with the actual NCF material on the front and back side, respectively. First of all, one can notice that the repeatability forced by the periodic boundary conditions leads to an appropriate reproduction of the tow architecture. Moreover, distortions induced by the perforation of the fibrous mat as defined by Loendersloot et al. [15] are observable in the form of "channels" along the fibers. This correlates well with the actual architecture of the NCF and more generally for 0°/90° biaxial NCF. Furthermore, although the simulation results reproduce well the zigzag shape of the loops on the back face of the material, the modeled fibers remain straight and parallel to each other. This is consistent with the assumed periodicity of the material at the scale of the fibers as described in Section 2. Therefore the model is not able to reproduce the waviness observed on the back face of the material. However, the diameter of the stitching yarn is reduced compared to the studied material. This is necessary to respect the length to diameter ratio imposed by the simulation software to avoid spurious self-contact calculation, while allowing an accurate representation of the inter-stitch interaction.

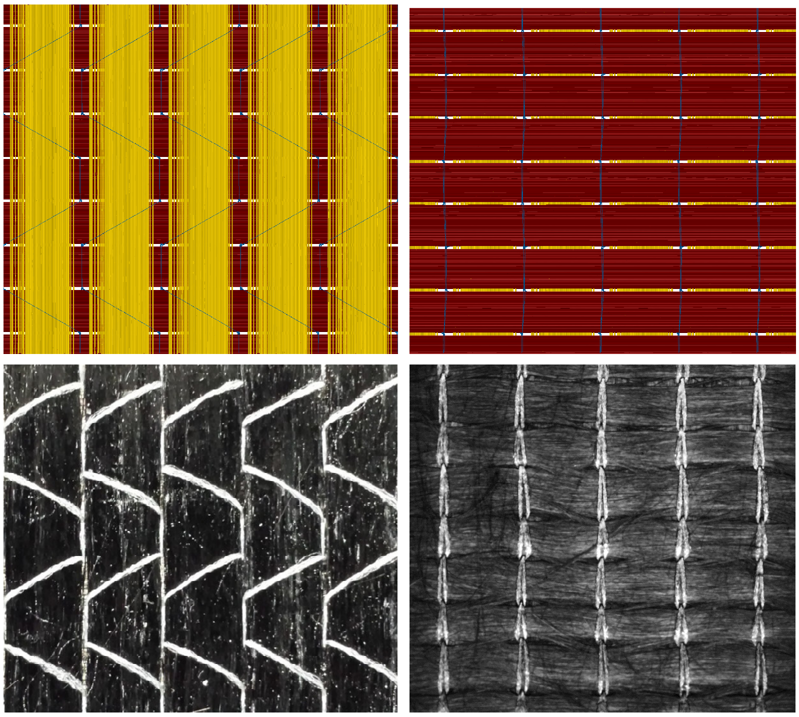

Figure 4. Comparison of the virtual "as-manufactured" geometry (top) and the studied non-crimp fabric (bottom).

4. Virtual characterization

In the following subsections the mechanical behavior of the virtual material is studied for out-of-plane compaction and shear deformation. These results are compared to experimental characterization results. The virtual characterization is performed on a reference simulation model with digital chain diameters of 69 µm.

4.1. Compaction

The out-of-plane compaction behavior of the 0°/90° biaxial NCF was tested with a rheometer produced by Anton Paar GmbH. In this test setup, one layer of the biaxial NCF is placed between two opposite plates that are subsequently closed with a constant velocity of 10 µm/s at room temperature. The applied pressure is recorded depending on the distance between the plates as illustrated in Fig. 5a). A thickness of 0.44 mm is measured at the maximum applicable pressure of 18 kPa, corresponding to a FVF of 38%.

The test conditions are reproduced in the simulation to compare the compaction behavior: two rigid plates are modeled and closed to generate the compaction of the material. The applied pressure depending on the distance between the plates is compared to the experimental results in Fig. 5a). The simulation results at a FVF of 38% and 67% are illustrated in Fig. 5b) and Fig. 5c) respectively.

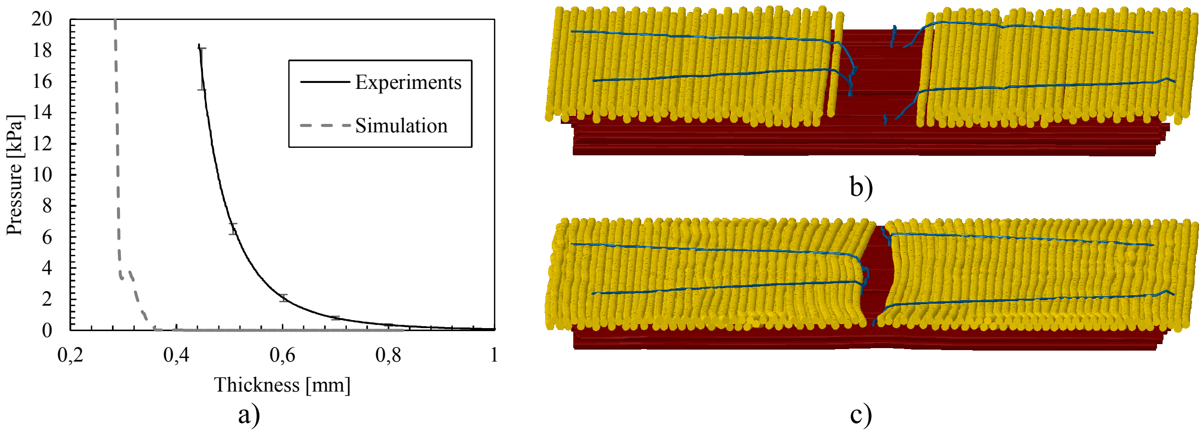

Figure 5. Comparison of the experimental and virtual compaction characterization a), and simulation results at 38% FVF b) and 67% FVF c).

The compaction behavior measured in the simulation differs significantly from experimental results. Based on a compaction pressure of 1.0 kPa, which is recommended in the standard DIN ISO 5084 for the thickness measurement of dry textiles, the thickness of the biaxial NCF is measured experimentally to 0.68 mm whereas the simulation result indicates a thickness of only 0.34 mm. Moreover, the progressive increase of the compaction pressure observed for a thickness smaller than 0.8 mm is not reproduced in the simulation: a sudden increase of the pressure is reached. This difference in thickness is explained due to the perfect alignment of the fibers in the simulation that enables a high FVF before any compaction force is required. In reality, the fibers do not lay perfectly parallel to each other and their interlacing prevent a perfect packing. Moreover, the diameter of the digital chain elements is calculated to achieve the same volume as the observed material. This assumes that the digital chains have an internal FVF of 100%, which is only correct when each filament is modeled. However, since many filaments are grouped in one chain, the FVF cannot exceed 92% (maximum FVF reached with a tight pack). Therefore, a finer discretization of the fibrous mat would lead to a more realistic behavior but involves a very high computation time. Further study should be performed on a realistic FVF to be assumed in the digital chains in order to increase the accuracy of the model with reduced computation costs.

4.2. Shear deformation

The experimental characterization of the shear behavior was performed with a picture frame testing rig at room temperature. The crosshead displacement is defined to 100 mm/min and the samples used for this study have a side length L_f of 175 mm. The filaments in the arms perpendicular to the clamped fibers have been removed to reduce their contribution in the measured shear force, as presented in [7]. Moreover, a predefined tension of 22 N/m is applied to the fibers before clamping. The test results averaged on 6 samples and normalized with respect to the sample side length are illustrated in Fig. 6a).

A pure shear deformation is applied to the unit cell in order to reproduce the experimental conditions with a constant shear deformation rate of 9 °/s. Boundary conditions are set to the model using Multi Point Constraints (MPC) to ensure an overall shear deformation of the unit cell while releasing the displacement of the constrained nodes along the edge of the deformed unit cell. The deformed finite element model of the unit cell is illustrated at 22.5° and 45° in Fig. 6b) and Fig 6c) respectively

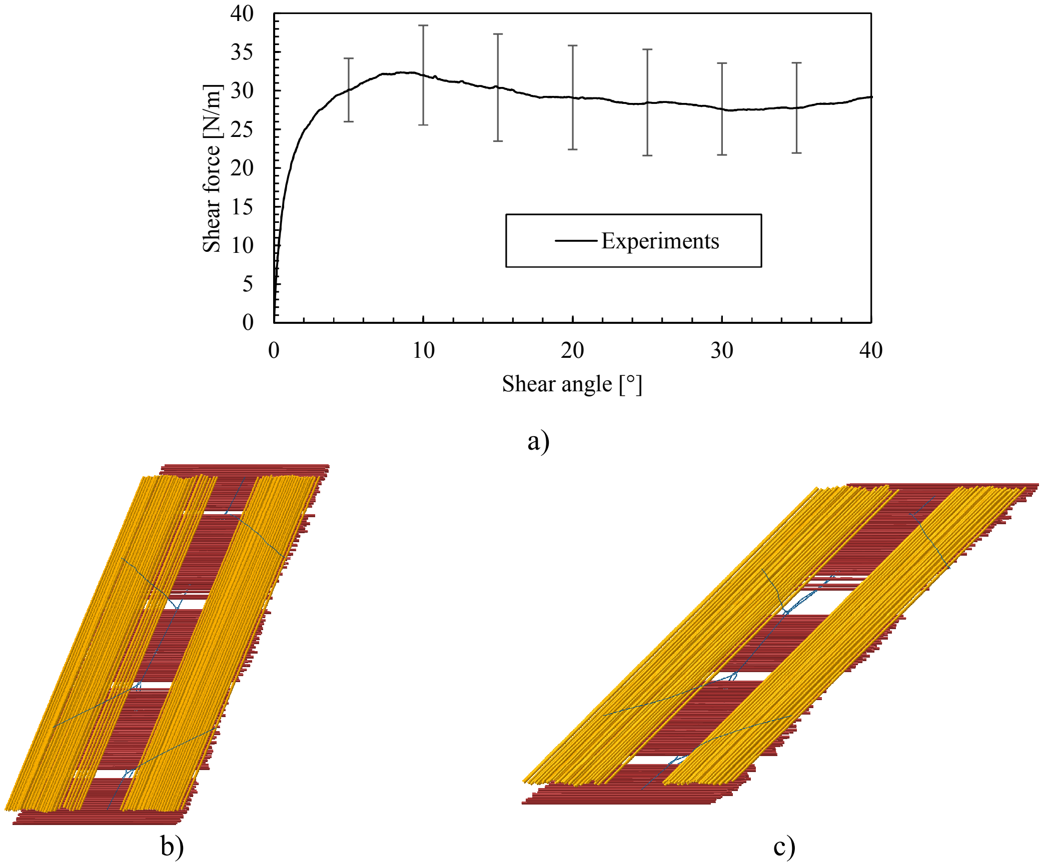

Figure 6. Experimental results of the picture frame shear tests a), and simulation results at 22.5° b) and 45° c) shear angle.

Although the deformation kinematic is accurately reproduced in the simulation, the forces required to shear the virtual textile up to a shear angle of 45° do not exceed 0.6 N/m in the simulation. This is almost 50 times smaller than those measured experimentally. Again, the difference can be explained by the perfect alignment of the fibers. Since the interactions are modeled with a coulomb friction, the frictional forces only depend on the contact pressure. Therefore, the friction occuring in the simulation is only induced by the tension in the stitching yarn. This leads to reduced inter-fiber interactions compared to the interaction resulting from the fiber interlacing observable in the studied material.

5. Conclusion and outlook

A virtual description of a biaxial 0°/90° biaxial NCF has been presented based on the periodicity of the textile architecture and modeled with multi-chain digital elements. The numerical approach reproduces the needle penetration of a homogeneous fibrous mat reasonably, while the geometry of the stitching yarns is idealized and subsequently contracted to reach a "as-manufactured" geometry. The mechanical response of the unit cell under compaction and in-plane shear has been tested and compared to experimental data. First, the compaction of the virtual NCF shows that the fibers can rearrange into a tightly packed configuration before any significant compaction force is achieved. Moreover, the shear deformation results from sliding of the digital chains. Since they are parallel aligned the resulting frictional forces are low. Due to these shortcomings, an insufficient correlation between numerical and experimental results has been obtained.

Future work will focus on an improved tow modeling including interlacing of filaments, alternative discretization and adapted friction coefficients.

6. Acknowledgment

The authors acknowledge KDX Europe Composites R&D Center GmbH for the financial and technical support of this study. The authors also acknowledge the French-Bavarian Academic Cooperation Center (BFHZ) for their financial funds essential for the collaboration with the research partners.

References

[1] Lomov SV, Barburski M, Stoilova T, Verpoest I, Akkerman R, Loendersloot R et al. Carbon composites based on multiaxial multiply stitched preforms. Part 3: Biaxial tension, picture frame and compression tests of the preforms. Composites Part A: Applied Science and Manufacturing 2005;36(9):1188–206.
[2] Cherif C. Textile Werkstoffe für den Leichtbau: Techniken-- Verfahren-- Materialien-- Eigenschaften. Heidelberg: Springer; 2011.
[3] Krieger H, Gries T, Stapleton SE. Design of Tailored Non-Crimp Fabrics Based on Stitching Geometry. Appl Compos Mater 2017;38(7):1655.
[4] Creech G, Pickett AK. Meso-modelling of Non-Crimp Fabric composites for coupled drape and failure analysis. J Mater Sci 2006;41(20):6725–36.
[5] Colin D, Bel S, Hans T, Hartmann M. On the Inter-Stitch Interaction in Biaxial Non-Crimp Fabrics. University of Palermo, Italy; 23th-25th 2018.
[6] Harrison P, Yu W, Long AC. Modelling the deformability of biaxial non-crimp fabric composites. In: Lomov SV, editor. Non-Crimp Fabric Composites: Elsevier; 2011, p. 144–65.
[7] Peng XQ, Cao J, Chen J, Xue P, Lussier DS, Liu L. Experimental and numerical analysis on normalization of picture frame tests for composite materials. Composites Science and Technology 2004;64(1):11–21.
[8] Green SD, Long AC, El Said B, Hallett SR. Numerical modelling of 3D woven preform deformations. Composite Structures 2014;108:747–56.
[9] Cichosz J. Experimental Characterization and Numerical Modeling of the Mechanical Response for Biaxial Braided Composites.
[10] Thompson A, El Said N, Such M, Belnoue J, Hallett S.R. Discrete modelling of Non-Crimp Fabric multi-layer preforming process. Texcomp-12 Conference, Raleigh, NC, USA 2015.
[11] Zhou G, Sun X, Wang Y. Multi-chain digital element analysis in textile mechanics. Composites Science and Technology 2004;64(2):239–44.
[12] Huang L, Wang Y, Miao Y, Swenson D, Ma Y, Yen C. Dynamic relaxation approach with periodic boundary conditions in determining the 3-D woven textile micro-geometry. Composite Structures 2013;106:417–25.
[13] Durville D. Simulation of the mechanical behaviour of woven fabrics at the scale of fibers. Int J Mater Form 2010;3(S2):1241–51.
[14] Lomov S, Belov E, Bischoff T, Ghosh S, Truong Chi T, Verpoest I. Carbon composites based on multiaxial multiply stitched preforms. Part 1. Geometry of the preform. Composites Part A: Applied Science and Manufacturing 2002;33(9):1171–83.
[15] Loendersloot R, Lomov SV, Akkerman R, Verpoest I. Carbon composites based on multiaxial multiply stitched preforms. Part V: geometry of sheared biaxial fabrics. Composites Part A: Applied Science and Manufacturing 2006;37(1):103–13.